

On the nonlinear behavior of r.c. buildings in near-field areas

Mariella Diaferio, Dora Foti

Abstract— The paper shows the results of a nonlinear dynamic analysis performed on a fixed base reinforced concrete 2D frame subject to near-field earthquakes, i.e. seismic motions close to the epicentral area of the fault rupture. In these areas both the acceleration and velocity signals are impulsive-type and, consequently, the response of the structures requires a specific study. The r.c. frame here considered has six levels and two equal spans; it has been designed according to the instructions provided in Eurocode 2 exclusively under gravity loads, the same design as for lots of existing buildings. The nonlinearity of the frame has been assumed with a diffuse plasticity and a fiber modeling has been considered for the structural elements.

Keywords— Near-field motions, nonlinear dynamic analysis, reinforced concrete frame, fiber modeling, damage index, ductility demand.

I. INTRODUCTION

AFTER the devastating earthquakes occurred in Northridge, Kobe, Kokaeli, Chi-Chi, etc., scientists increased the interest towards earthquake effects on structures due to the many collapsed buildings and consequent important human lost.

From the many records at different locations on the territories, it was realized that near-field motions are significantly different from those usually recorded in far-field areas. Usually, near-field records are referred to those signals recorded within an area of few kilometers (maximum 25 Km) around the projection on the earth surface of the fault. From this, the importance and necessity to better know the behavior of such inputs for structures.

In near-field areas the component of motion normal to the fault line is impulsive, with a high pulse period in acceleration. Therefore, it is clear the importance of considering the effects of near-field earthquake in structural design.

Unfortunately, some codes (like the Italian Code, NTC 2008 [1-2]) only refer to the seismic design in far-field or intermediate areas, where the characteristics of the ground

This work was supported in part by PRIN-MIUR 2010 research project entitled "Dynamics, Stability and Control of Flexible Structures" and in part by the funding by the European Territorial Cooperation Programme "Greece-Italy 2007-2013", project Structural Monitoring of ARTistic and historical BUILDing Testimonies (S.M.ART:BUIL.T.).

Mariella Diaferio, Department of Civil Engineering and Architecture, Technical University of Bari, Bari, Italy

Dora Foti, Department of Civil Engineering and Architecture, Technical University of Bari, Bari, Italy.

motion are quite known. But the current way of structural analysis based on far-field recorded motions cannot be used to describe the phenomena in near-field areas.

The main differences between the motions recorded in near-field areas respect to far-field ones can be briefly summarized as follows:

- The direction of propagation of the fault has a major influence in near-field areas as the stratification of soil has minor effects. On the contrary, in far-field areas, the soil stratification and the site conditions are of primary importance for the horizontal components of the seismic waves;

- In near-field areas the acceleration ground motion shows a pulse in the field of low frequencies and a pronounced pulse in the time-history diagrams of velocity and displacement. In this case the motion has a short duration. On the contrary, in far-field areas, the recordings of acceleration, velocity and displacement have the characteristics of cyclic motions, with a "long" duration of the action;

- In near-field areas the velocity reaches peak values; in such areas, in fact, the velocity appears to be the most significant parameter in the design, replacing the acceleration, which represents the most significant parameter in the design in far-field areas.

Studies have also been conducted on the response of buildings in near-fault areas protected with dissipaters [3-4], or with base isolation systems [5-6] and with energy dissipaters [7-11]. New solutions for the seismic protection in such areas have been also proposed [12-15]; provisions may be introduced for increasing the protection of buildings in near-fault areas [16-18].

In the following, the response of a six-floor reinforced concrete frame is analyzed. The frame is subject to six different signals acquired at stations located in near-field areas and arranged in the direction of propagation of the fault. It was also performed an analysis of local seismic response, assuming a stratigraphic profile, which has allowed to understand the influence of site effects on near-field earthquakes. The nonlinear dynamic analysis has been carried out by means of Sismostruct_v7 software [19] on r.c. frames assuming a diffuse plasticity and fiber modeling of the structural elements.

II. DESCRIPTION AND MODELING

The behavior of a reinforced concrete framed building fully fixed at the base is here described. The geometrical characteristics of the structure are shown in Fig. 1, the frame

has a total height of 19 m and a width of 12 m. The frame, which is symmetric with respect to the central column, is made up of six floors (each floor is 3 m high), and two equal 6 m spans. It has been designed according to the Eurocode 2 instructions [20] exclusively under gravity loads, as the most common existing buildings. All the beams have a rectangular cross section with the same dimensions: base $b = 30$ cm and height $h = 40$ cm, while the transversal section of the columns is variable with the height (Fig. 1). The dimensions of such sections are shown in Table 1.

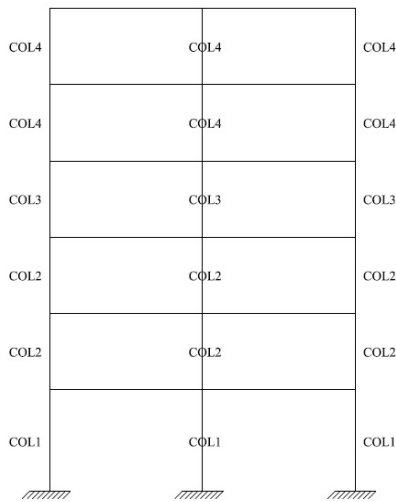


Fig. 1. Reinforced concrete frame utilized in the analysis.

Each beam is subject to a uniformly distributed load with

the unitary loads obtained from NTC 2008 $G_{k1}=17$ KN/m, $G_{k2}=16$ KN/m, $Q_k=10$ KN/m [1-2]. The load combination at the Ultimate Limit State (ULS) has been defined in accordance with the same current code and consists of a load uniformly distributed on all the beams of the structure: $Q_d=61$ KN/m ($Q_d=1.3 \cdot G_{k1}+1.5 \cdot G_{k2}+1.5 \cdot Q_k$).

	BASE [cm]	HEIGHT [cm]
COL1	60	30
COL2	50	30
COL3	40	30
COL4	30	30

Table 1. Dimensions of the cross section of the columns.

The reinforcement design and the check of the sections' dimensions were performed in accordance to Eurocode 2 (gravitational regime); in particular, it is employed C25/30 concrete and B450C steel [1].

The beams have been reinforced adding the following bars:

- Supports at the edge: $A's=2\Phi 18+4\Phi 20$, $A_s=2\Phi 18+2\Phi 20$;
- In the center of the beam: $A's=2\Phi 18$, $A_s=2\Phi 20$;
- Central support: $A's=2\Phi 18+6\Phi 20$, $A_s=4\Phi 18$.

where $A's$ and A_s are the reinforcements at the upper and lower side of the cross section, respectively.

In Fig.2 the reinforcement adopted for all the beams of the structure is shown.

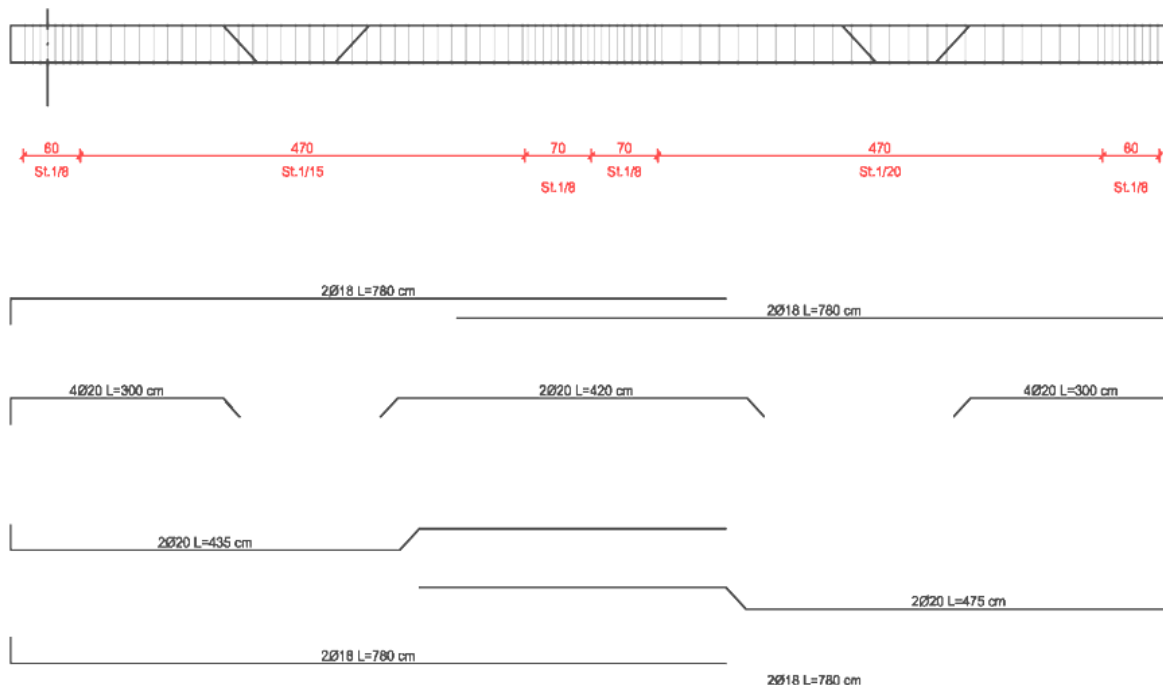


Fig. 2. Beam reinforcement.

Table 2 shows the period and frequency values of the first four natural modes and the related participating masses.

Fig. 3 shows the four modal shapes of the frame.

Mode	Period [s]	Frequency [Hz]	Participating mass [%]
1	1.86	0.5376	86
2	0.63	1.5873	9.5
3	0.35	2.8571	2.7
4	0.24	4.1667	1

Table 2. Dynamic characteristics of the frame in Fig. 1.

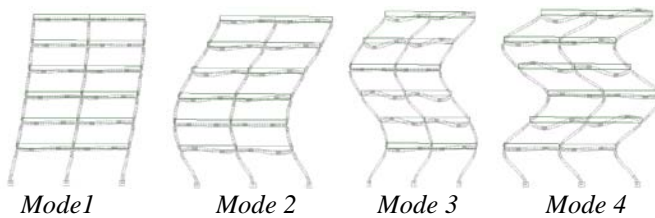


Fig. 3. Mode shapes of the frame in Fig. 1.

The non-linear dynamic analysis of the frame has been carried out by means of Sismostruct_v7 software [18] and adopting the following constitutive models:

1 - Model of Mander et al. for concrete [21]: it is a uniaxial nonlinear model with a constant constraint for concrete, at the beginning proposed by Madas [21], which follows the constitutive law proposed by Mander et al. [22] and the cyclic laws proposed by Martinez-Rueda and Elnashai [23]. The effects of confinement due to the transversal reinforcements are included assuming a constant confining pressure through the entire stress-strain law (Fig. 4, Table 3). The confining pressure has been evaluated as a function of the geometry, the step and the stirrups' diameter; as a result this pressure improves the stress-ultimate strain behavior of the material and, consequently, of the section;

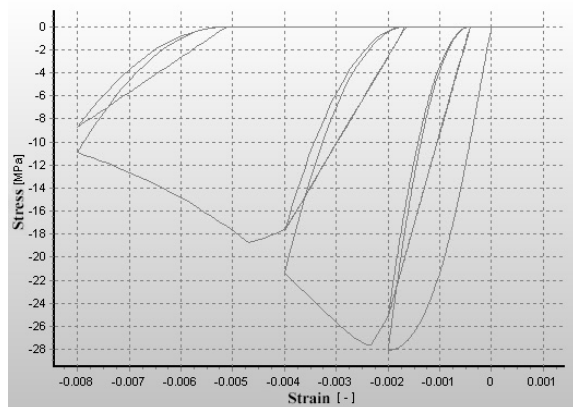


Fig. 4. Stress-strain relationship for concrete.

Compressive strength	Tensile strength	Deformation at the peak value of the stress	Density
[Pa]	[Pa]	[m/m]	[N/m ³]
$3 \cdot 10^7$	0	0.002	24000

Table 3. Mechanical characteristics adopted for concrete.

2 - Model of Menegotto-Pinto for steel [24]: It is a uniaxial model first proposed by Yassin [24] on the basis of a simple but efficient stress-strain relationship proposed by Menegotto and Pinto [25], and then enriched by the isotropic hardening laws proposed by Filippou et al. [26]. Its use should be limited to the modeling of the behavior of reinforcements in r.c. structures, especially those subject to complex loadings histories with significant load reversals (Fig. 5, Table 4).

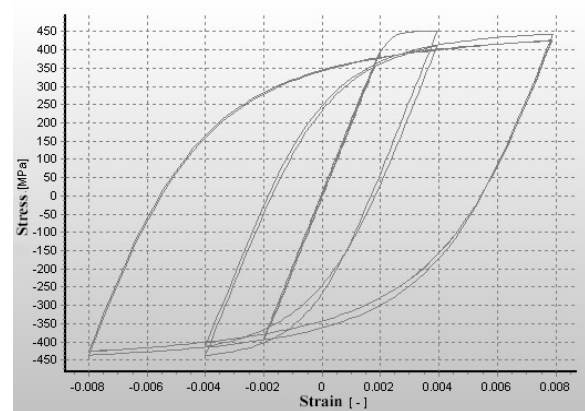


Fig. 5. Stress-strain relationship for steel.

Modulus of elasticity	Yielding strength	Parameter of hardening	Density
[Pa]	[Pa]	[-]	[N/m ³]
$2 \cdot 10^{11}$	$4.5 \cdot 10^8$	0.005	78000

Table 4. Mechanical characteristics adopted for steel.

For the non-linear analysis the so-called "plasticity widespread" modeling was implemented, i.e. the beam/column element is divided into elements "FIBERS" (Fig. 6) that is one-dimensional elements with a non-linear constitutive law. The stress-strain state of a section is obtained by integration of the uniaxial non-linear stress-strain response of each fiber.

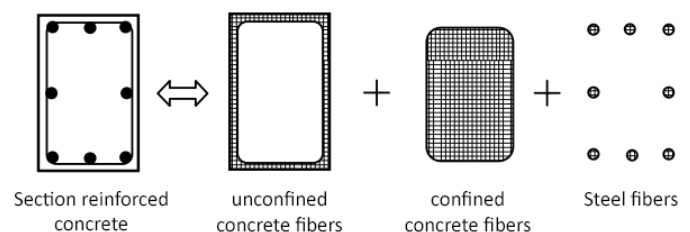


Fig. 6. Discretization in fibers of a r.c. section [27].

Therefore, appropriately subdividing each structural element, it is possible to accurately describe the development of the plastic hinges in the element without the need of assuming them 'a priori'. The limit of this modeling approach, as well as the computational effort, is due to the inability to catch any effect of the shear forces.

III. NEAR-FIELD EARTHQUAKES

The analysis of near-field motions shows that, in cases where the fracture generated from seismic shock propagates with a speed close to that of the shear waves, most of the energy released during the earthquake produces, at the beginning of the phenomenon and for a short duration, a pulse of high intensity. This strong impulse is mainly visible in the component of motion along the direction perpendicular to the fault line. Consequently, the velocity and displacement motion time histories along the direction of propagation of the fault are characterized by pulses with high amplitude. On the contrary, the motion recorded in the opposite direction, does not show impulsive characteristics. Moreover, the peak value of the velocity along the direction of the fault propagation is even three times larger than that relating to the component of motion in the orthogonal direction. In addition, the peak values of the acceleration and displacement are higher.

For the dynamic analysis of the examined structure the following six near-field accelerograms have been considered:

- Duzce-Turchia, November 1999; accelerogram recorded in Duzce;
- Kobe, 1995; two accelerograms recorded respectively in Kobe-JMA and in Takatori;
- Northridge 1994; two accelerograms recorded respectively in Rinaldi and Sylmar;
- Kokaeli, August 1999 recorded in Yarimka.

In the analysis the components at 90° or impulsive-type of the near-field signals are considered. In order to compare the dynamic results, the accelerograms on the bedrock have been scaled to a peak value of the acceleration of 0.1g, obtaining the acceleration response spectra of Fig. 7.

The study has been centered on the local seismic response, utilizing the EERA calculus sheet [28] to estimate the effects of the seismic signals on the stratigraphic profile under the foundations adopted for the analysis and shown in Fig. 8.

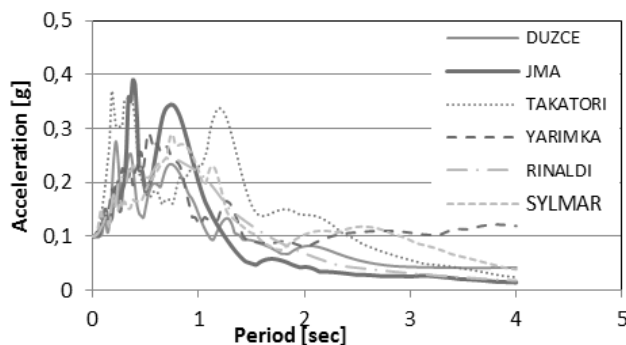


Fig. 7. acceleration Response spectra of the examined six near-field earthquakes at the bedrock.

In Fig. 9 the acceleration time-histories of the not-filtered and filtered signals are reported for Duzce-Duzce earthquake record.

It is possible to notice that the time-histories are quite similar; however, the spectra show high differences due to the filtering: the signal recorded on outcrop shows a higher response.

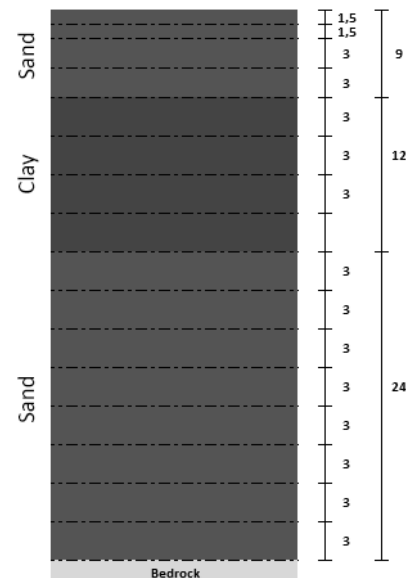


Fig. 8. Stratigraphic profile of the foundation soil.

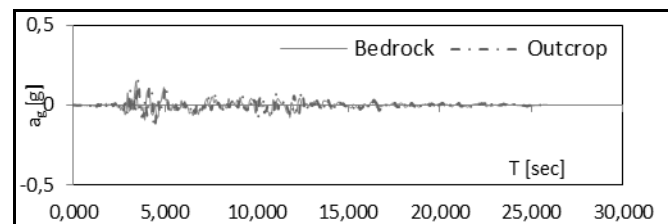


Fig. 9. Acceleration time-histories of Duzce-Duzce earthquake at the bedrock (continuous line) and at the foundation level (dashed line) in accordance with the stratigraphic profile in Fig. 8.

Fig. 10 shows the acceleration spectra of the Duzce-Duzce earthquake evaluated at the bedrock and at the foundation level, this one has been estimated in accordance with the stratigraphic profile in Fig. 8. It can be observed that the spectra at the foundation level is higher than the one at the bedrock for low period values; in this period range it can be found the periods of the natural modes of the examined frame higher than the first.

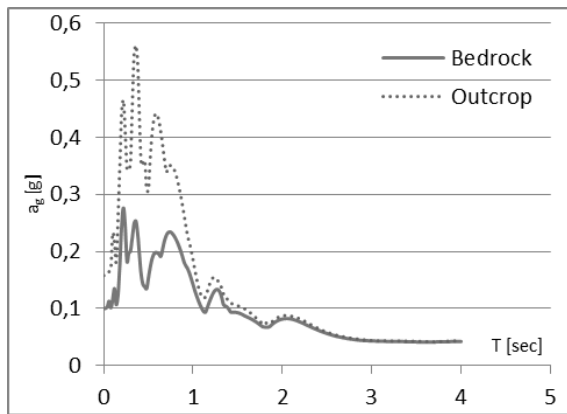


Fig. 10. Comparison between the acceleration spectra at the bedrock and at the foundation level for Duzce-Duzce earthquake.

IV. NONLINEAR DYNAMIC ANALYSIS

In the present section the results of the performed nonlinear dynamic analysis are summarized.

A. Damage index

The damage index is defined as the ratio between the maximum displacement of the structure and its total height. The histogram in Fig.11 shows that the Takatori accelerogram produces the worse effect on the r.c. frame, while Duzce accelerogram induces the minimum effect. It is an expected result since Duzce accelerogram presents the lowest acceleration peak at the foundation level.

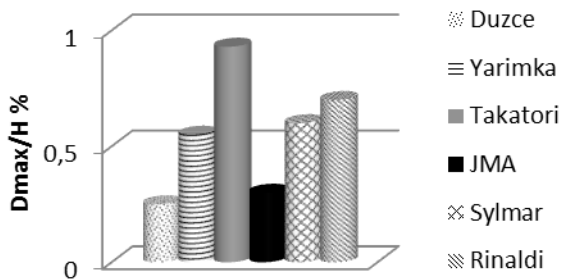


Fig. 11. Damage Index of the r.c. frame in Fig. 1.

B. Amplification

The amplification, i.e. the ratio between the maximum acceleration evaluated at the top floor and the maximum ground acceleration, reaches its maximum value for the Takatori signal (Fig. 12): in fact, in this case the maximum acceleration at the top of the frame is 0.205g. This result agrees with the acceleration response spectra in Fig. 7 that shows the higher values nearest the first period of the frame and also in the range of period where the higher natural modes of the frame are located. More consistent amplifications were found for Yarimka and Rinaldi earthquakes, followed by JMA. Not excessive amplifications were suffered during Duzce and Sylmar signals.

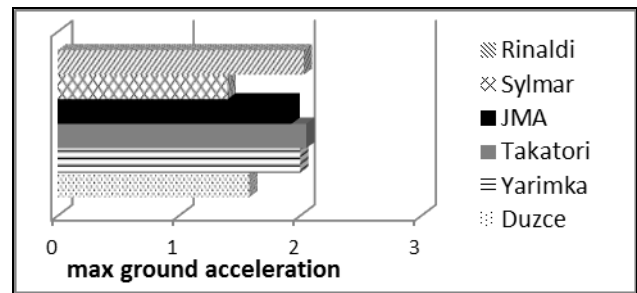


Fig. 12. Maximum amplifications of the frame of Fig. 1.

C. Shear force at each floor

Fig. 13 shows the results obtained for the maximum shear force at each floor of the examined frame for each input signal. It is noticed that, in general, shear stress usually reduces from the lower floors to the higher ones.

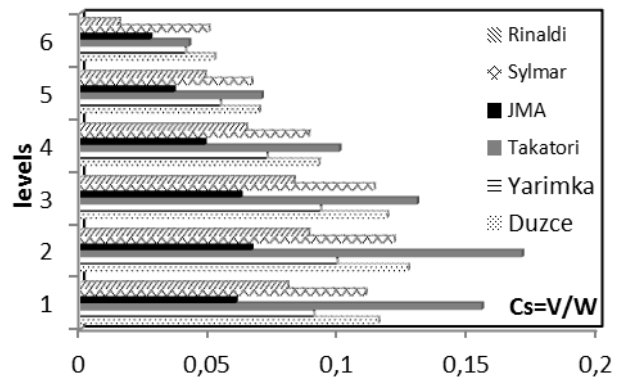


Fig.13. Shear force at each level of the frame.

It is not the case for the first and second levels. At the second level, in fact, there is a change in the interstory level, which reduces from the first level to the second and the following ones. There is an increase in deformability and it occurs for all the signals due to the sudden change of the geometry of the elements. In fact, the sudden increment in stiffness from the 1st to the 2nd level can produce this effect.

D. Interstory drifts

The plot in Fig. 14 shows the interstory drifts, i.e. the ratio between the maximum displacement and the interstory height, for each level of the frame.

The interstory drifts are quite constant along the height of the frame except the ones related to the Takatori earthquake for which the higher values are recorded at the 2nd- 3rd and 4th level; this behavior may be due to the influence of the higher modes of the frame.

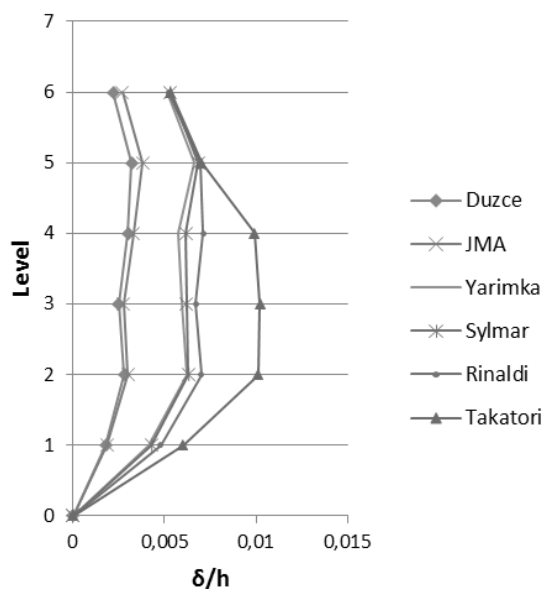


Fig. 14. Interstory drifts at each level of the frame.

E. Ductility demand

In Fig. 15 the values of the maximum rotations at the beam ends are plotted for each level: this value is an index of the ductility demand of the structure.

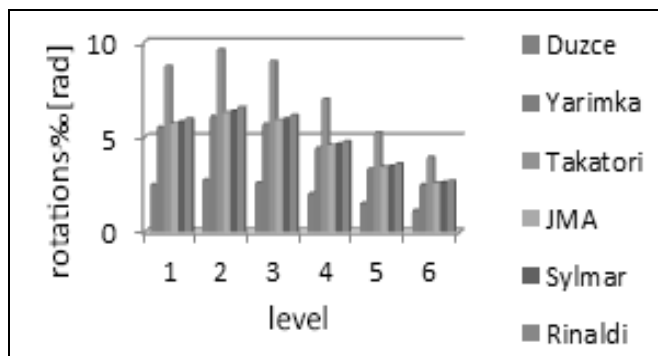


Fig. 15. Ductility demand.

The highest values of ductility demand are obtained for Takatori accelerogram. The demand tends to decrease at the higher levels of the structure with the exception of the first and second levels.

Focusing the attention on the framed structure, it should be noted that, due to the seismic action, various failure mechanisms may appear in relation to the dimensions of the sections of the structural elements. Each one of these mechanisms is characterized by a different level of ductility and not all of them are associated with adequate ductility levels. Therefore, in the design the proportioning of the structural elements is carried out so as not to activate the mechanisms of collapse that, not ensuring the overall ductility demand, would make the structure inadequate to the design earthquake.

In Fig. 16, in fact, the failure is observed only in the columns (darker color close to the nodes), while no section of

the beams reaches the failure. This result is obtained for all the earthquake signals utilized in the present research. This mechanism of weak columns and strong beams is not aimed because it is a low ductile behavior with a limited dissipative capacity of the frame

V. CONCLUSIONS

This paper shows the results of a nonlinear dynamic analysis of a fixed base reinforced concrete frame to the action of near-field earthquakes, i.e. close to the epicentral area of the fault rupture.

The r.c. frame has six levels and two equal spans; it has been designed according to the instructions provided in the Eurocode 2 exclusively under gravity loads.

Six near-field ground motions have been considered; their peak accelerations at the bedrock have been scaled to a peak value of 0.1g. Subsequently, assuming a stratigraphic profile, it was performed a mono-directional analysis of the seismic response, which allowed to obtain the seismic signals at the foundation level of the structure.

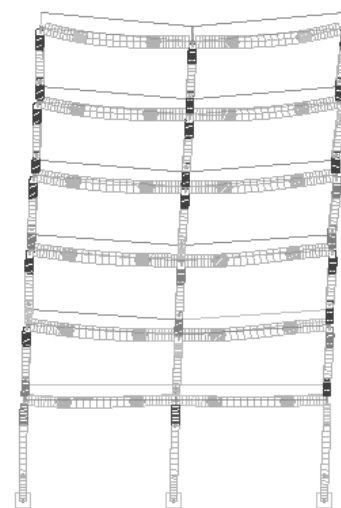


Fig. 16. Final deformation during Yarimka earthquake signal for the frame sited on the outcrop.

From the results it has been possible to conclude that the nodal areas show plasticization when subjected to unfiltered signals, while when considering the effect of the soil and its stratigraphy the nodal areas are affected by real cracks and failure.

As evidenced in par. 4.5, failure is observed only in the columns while no section of the beams reaches the failure. Of course, the behavior recorded is a sign of bad behavior since the collapse does not involve different parts of the overall structure and focuses the inelastic deformations at the ends of the beams of all floors and at the base of columns (mechanism of weak columns and strong beams). A low ductile behavior and a limited dissipative capacity of the frame is deduced, given the low plastic strains exhibited before failure. This

behavior is caused by an increased ductility demand as a result of the strong impulsive nature of the seismic force caused by high velocities in near-field areas. Also for this reason the need to develop a method to evaluate the ductility as a function of the velocity of the seismic action represents a significant aspect to be developed in future research in this field.

ACKNOWLEDGMENT

The authors acknowledge the funding by PRIN-MIUR 2010 research project entitled “Dynamics, Stability and Control of Flexible Structures” and the funding by the European Territorial Cooperation Programme “Greece-Italy 2007-2013”, project Structural Monitoring of ARTistic and historical BUILDing Testimonies (S.M.ART. BUIL.T.).

REFERENCES

- [1] *Nuove norme Tecniche per le Costruzioni* – Decreto del Ministero delle Infrastrutture 14 gennaio 2008 (in Italian).
- [2] *Circolare n. 617, 2 febbraio 2009*, Istruzioni per l’applicazione delle “Nuove norme tecniche per le costruzioni” di cui al decreto ministeriale 14 gennaio 2008, Gazzetta Ufficiale n.47 del 26-2-2009 Suppl. Ordinario n. 27, Roma (in Italian).
- [3] W.-L. He, A.K. Agrawal, “Analytical model of ground motion pulses for the design and assessment of seismic protective systems”, *Int. J. of Struct. Eng.*, vol.134, no.7, 2008, pp.1177-1188.
- [4] D. Foti, “Response of frames seismically protected with passive systems in near-field areas”, *Int. J. of Struct. Eng.*, 2014, vol. 5, no. 4, 2014, pp. 326-345.
- [5] R. Greco, G. Marano, D. Foti, “Strong motion duration effects on base isolated systems”, *Physica A - Statistical Mechanics And Its Applications*, vol. 274; no.1-2, 1999, Amsterdam, North Holland. PII: S 0378-4371(99)00311-8.
- [6] F. Mazza, M. Mazza, “Nonlinear modeling and analysis of r.c. framed buildings located in a near-fault area”, *The Open Constr. & Build. Tech. J.*, vol. 6, 2012, pp.346-354.
- [7] L. Tirca, D. Foti, M. Diaferio, “Response of middle-rise steel frames with and without passive dampers to near-field ground motions”, *Eng. Struct.*, vol.25, no.2, 2003, pp.169-179.
- [8] Z. Xu, A.K. Agrawal, W.-L. He, P. Tan, “Performance of passive energy dissipation systems during near-field ground motion type pulses”, *Eng. Struct.*, vol.29, no.2, 2007, pp.224-236.
- [9] M. Dicleli, A. Mehta, “Effect of near-fault ground motion and damper characteristics on the seismic performance of chevron braced steel frames”, *Earthq. Eng. and Struct. Dyn.*, vol.36, no.7, 2007, pp.927-948.
- [10] D. Foti, “On the seismic response of protected and unprotected middle-rise steel frames in far-field and near-field areas”, *Shock and Vib.*, vol. 2014, 2014, Article ID 393870.
- [11] D. Foti, “Local ground effects in near-field and far-field areas on seismically protected buildings”, *Soil Dyn. and Earthq. Eng.*, vol. 74, 2015, pp.14-24.
- [12] D. Foti, R. Nobile, “Optimum design of a new hysteretic dissipater”, In: Lagaros N, Plevris V, Mitropoulou C, editors. *Design Optimization of Active and Passive Structural Control Systems*, Hershey PA: ICI Global, 2012, pp. 274-299. <http://www.igi-global.com/book/design-optimization-active-passive-structural/64896>. ISBN: 978-146662029-2; doi: 10.4018/978-1-4666-2029-2.ch012.
- [13] D. Foti, M. Diaferio, R. Nobile, “Dynamic Behavior of New Aluminum-Steel Energy Dissipating Devices”, *Structural Control and Health Monitoring*, Vol.20, No.7, 2013, pp.1106-1119. ISSN:154-5225.
- [14] D. Foti, M. Diaferio, R. Nobile, “Optimal design of a new seismic passive protection device made in aluminium and steel”, *Struct. Eng. and Mech.s*, vol.35, no.1, 2010, pp.119-122.
- [15] Corbi, O., Zaghw, A.H., Elattar, A., Saleh, A., “Preservation provisions for the environmental protection of egyptian monuments subject to structural vibrations”, *Int. J. Mechanics*, 2013, Vol.7(3), pp. 172 – 179, ISSN 1998-4448.
- [16] Baratta A., Corbi O., Contribution of the fill to the static behaviour of arched masonry structures: Theoretical formulation, *J. Acta Mechanica*, Vol. 225, No.1, 2014, pp. 53-66, doi: 10.1007/s00707-013-0935-x.
- [17] Baratta, A., Corbi, I., Corbi, O., Bounds on the Elastic Brittle solution in bodies reinforced with FRP/FRCM composite provisions, *Journal of Composites Part B: Engineering*, vol. 68, 2014, pp. 230-236, doi: 10.1016/j.compositesb.2014.07.027.
- [18] Baratta, A., Corbi, I., Topology optimization for reinforcement of no-tension structures, *Journal of Acta Mechanica*, vol.225, No.3, 2014, pp. 663-678, doi: 10.1007/s00707-013-0987-y.
- [19] *Seismosoft, SeismoStruct v7.0 – A computer program for static and dynamic nonlinear analysis of framed structures*, 2014, available from <http://www.seismosoft.com>.
- [20] *CEN. Eurocode 2 – Design of concrete structures – Part 1: General rules and rules for buildings*, Brussels, 2005, EN 1992-1-1.
- [21] P. Madas, *Advanced Modelling of Composite Frames Subjected to Earthquake Loading*, PhD Thesis, Imperial College, University of London, London, UK, 1993.
- [22] J.B. Mander, M.J.N. Priestley, R. Park, “Theoretical stress-strain model for confined concrete”, *J. of Struct. Eng.*, vol. 114, no. 8, 1988, pp. 1804-1826.
- [23] J.E. Martinez-Rueda, A.S. Elnashai, “Confined concrete model under cyclic load”, *Mat. and Struct.*, vol. 30, no. 197, 1997, pp. 139-147.
- [24] M.H.M. Yassin, *Nonlinear analysis of prestressed concrete structures under monotonic and cyclic loads*, PhD Thesis, University of California, Berkeley, USA, 1994.
- [25] M. Menegotto, P.E. Pinto, “Method of analysis for cyclically loaded R.C. plane frames including changes in geometry and non-elastic behaviour of elements under combined normal force and bending”, *Symposium on the Resistance and Ultimate Deformability of Structures Acted on by Well Defined Repeated Loads*, International Association for Bridge and Structural Engineering, Zurich, Switzerland, 1973, pp. 15-22.
- [26] F.C. Filippou, E.P. Popov, V.V. Bertero, *Effects of bond deterioration on hysteretic behaviour of reinforced concrete joints*, Report EERC 83-19, Earthquake Engineering Research Center, University of California, Berkeley, 1983.
- [27] L. Petrini, R. Pinho, G.M. Calvi, *Criteri di Progettazione Antisismica degli edifici*, IUSS Press, 2004, ISBN: 88-7358-039-4.
- [28] J.P. Bardet, K. Ivhil, C. H. Lin, *EERA: A Computer program for Equivalent-linear Earthquake site Response Analysis of Layered soil deposits*, Department of Civil Engineering, University of Southern California, August 2000.